Journal of Material Cycles and Waste Management (2023) 25:650–661
https://doi.org/10.1007/s10163-022-01573-9

SPECIAL FEATURE: ORIGINAL ARTICLE

8th 3R International Scientific Conference (8th 3RINCs 2022)

Effects of heating rate and temperature on product distribution of poly-lactic acid and poly-3-hydroxybutyrate-*co*-3-hydroxyhexanoate

Zhuze Shao[1] · Shogo Kumagai[1,2] · Tomohito Kameda[1] · Yuko Saito[1] · Toshiaki Yoshioka[1]

Received: 9 August 2022 / Accepted: 6 December 2022 / Published online: 20 December 2022

Abstract
In this study, poly-lactic acid (PLA) and poly-3-hydroxybutyrate-*co*-3-hydroxyhexanoate (PHBH) were pyrolyzed at various temperatures (300, 350, 400, 500, 600, and 700 °C) and heating rates (5, 10, 20, 30, and 40 °C min^{-1}) using a pyrolysis–gas chromatograph/mass spectrometer (Py–GC/MS). The results revealed that the main pyrolysis products of PLA were acetaldehyde, lactide (including meso-lactide and D-, L-lactide), and oligomers. Crotonic acid and its oligomers accounted for most of the PHBH pyrolyzates. The pyrolysis temperature significantly correlated with the product distribution, but the heating rate had a small effect on the product distribution. Lactide and crotonic acid were two kinds of high-value chemicals, and their highest yields were obtained at 400 and 600 °C with 29.7 and 72.6 area %, respectively. Secondary reactions could not be neglected at 700 °C, and acetaldehyde and crotonic acid decreased to 65.0 and 69.6 area %, respectively. These results imply that pyrolyzate selectivity can be controlled by temperature management during pyrolysis.

Keywords Poly-lactic acid · Poly-3-hydroxybutyrate-*co*-3-hydroxyhexanoate · Pyrolysis · Temperature effects · Pyrolysis–gas chromatograph/mass spectrometer

Introduction

Plastics have become indispensable in modern society since they are commercially available. Over the past few decades, plastic production has steadily increased from 1.5 million tons in 1950 to 368 million tons in 2019 owing to its superior performance in stability, lightness, and low cost [1, 2]. However, the production and use of plastics have brought about a series of negative effects [3, 4], and the introduction of bioplastics is a promising way to reduce the environmental burden. Bioplastics are generally divided into three types: bio-based/non-biodegradable, petroleum-based/biodegradable, and bio-based/biodegradable plastics. Of these, bio-based/biodegradable plastic is the most remarkable, as it consumes less petroleum in the process of production and can be broken down by microorganisms when discarded. Many countries have introduced policies to encourage the use of bioplastics [5, 6], and the global biodegradable plastics production is forecasted to increase from 1.23 million tons in 2020 to 1.8 million tons in 2025, of which poly-lactic acid (PLA) will be the most utilized bioplastics, and poly-hydroxy alkanoate (PHA) production is expected to increase greatly [7].

However, some researchers pointed out that it is not a silver bullet to prevent plastic pollution [8, 9]. Generally, the degradation rate of biodegradable plastics is extremely slow. Depending on the types, it may take months or even years for bioplastics to degrade [10, 11]. Additionally, plastics form microplastics during biodegradation, which can be absorbed by soil organisms or transported to aquatic ecosystems [12]. Therefore, from an economic and ecological point of view, it would be better if biodegradable plastics could be recycled as effectively as petroleum-based plastics.

✉ Shogo Kumagai
kumagai@tohoku.ac.jp

1 Graduate School of Environmental Studies, Tohoku University, 6-6-07 Aoba, Aramaki-aza, Aoba-ku, Sendai, Miyagi 980-8579, Japan

2 Division for the Establishment of Frontier Sciences of Organization for Advanced Studies, Tohoku University, 2-1-1 Katahira, Aoba-ku, Sendai 980-8577, Japan

Among the technologies for treating plastic waste, pyrolysis is promising and can rapidly convert waste plastics into chemical feedstock in an inert environment. Many researchers studied the pyrolysis of petroleum-based and non-biodegradable plastics, which can produce a wide range of gasses, oils, waxes, and solids [13, 14]. The types of feedstock, reactor, catalyst, pyrolysis temperature, residence time, and pressure are considered to be the main factors affecting the distribution of pyrolysis products [15–18]. Extensive research is conducted on the pyrolysis of bio-based biodegradable plastics, and it is reported that the main pyrolyzates of PLA are CO, CO_2, acetaldehyde, acetone, acrylic acid, meso-lactide, and D-, L-lactide, and trans-esterification is considered to be the basic pyrolysis mechanism [19, 20]. The major pyrolysis products of poly-3-hydroxybutyrate (PHB) were crotonic acid and its oligomers, which were mainly formed via cis-elimination [20, 21]. Metal-based catalysts, such as Zn, Ti, and Sn, were reported to facilitate the pyrolysis of PLA [22, 23], and MgO, $Mg(OH)_2$ and CaO were used to improve the yield of crotonic acid in PHB pyrolysis [24, 25]. Temperature and heating rate are important factors affecting pyrolysis that may influence production composition [26]. At higher temperatures, stronger cracking of C–C bonds of plastic was observed, and higher gas yield was obtained [27, 28]. At lower heating rates, the slow conversion/degradation allows the volatiles to stay in the heating zone for an extended period, resulting in further cracking or reformulation of the hydrocarbons to form low carbon range hydrocarbons producing a low-density pyrolytic oil [29]. However, most of the studies focused on petroleum-based plastics, such as PE, PP, PS, PET, and PVC. There is little research on their influences on the pyrolysis of bioplastics. To understand the effects of temperature on product distribution, it is necessary to study the pyrolysis behavior of biodegradable plastics at different temperatures and heating rates. Additionally, the results can help to determine the best pyrolysis conditions for obtaining high-value chemicals.

Pyrolysis–gas chromatography/mass spectrometry (Py–GC/MS) is an effective analytical technique widely used for the characterization of polymers and analysis of plastics in the environment [30, 31]. It is also proven to be suitable for characterizing the degradation of bioplastics [32, 33]. Therefore, we prepared PLA and poly-3-hydroxybutyrate-*co*-3-hydroxyhexanoate (PHBH) as representatives to analyze the effect of the heating rate and temperature on the pyrolysis product distribution using Py–GC/MS. The pyrolysis kinetic parameters were also calculated using the model-free isoconversional method, and the reaction models were determined using the Criado master plot.

Materials and methods

Materials

PLA was purchased from Standard Testpiece Co. Ltd. (Kanagawa, Japan). PHBH (X131A) was supplied by Kaneka Co. Ltd. (Tokyo, Japan). All the samples were ground to a size of 100 mesh or less. The obtained samples were dried in a vacuum oven at 40 °C for over 12 h before the pyrolysis tests.

Thermogravimetric (TG) measurements and kinetic analysis

TG analysis (TGA) was performed using a TG analyzer (STA7200RV, Hitachi High-Tech Science Corporation, Japan). Approximately 5 mg of sample was heated from 50 to 700 °C at the rates of 5, 10, 20, 30, and 40 °C min^{-1} under nitrogen atmosphere at a flow rate of 100 mL min^{-1}.

The decomposition rate can be described as follows:

$$\frac{d\alpha}{dt} = k(T)f(\alpha), \tag{1}$$

where, $k(T)$ is the rate coefficient, $f(\alpha)$ is the differential conversion function depending on the reaction mechanism, and α is the conversion rate, which can be expressed as:

$$\alpha = \frac{m_0 - m_t}{m_0 - m_\infty}, \tag{2}$$

where, m_0, m_t, and m_∞ are the initial mass, mass at time t, and the final mass, respectively. In this study, all the samples were completely decomposed, and the weight barely changed when the heating program ended. Therefore, m_∞ was considered as the sample weight at 700 °C. The rate coefficient can be described by the Arrhenius equation:

$$k(T) = Ae^{-\frac{E_a}{RT}}, \tag{3}$$

where, A is the pre-exponential factor (min^{-1}), E_a is the activation energy (J), R is the universal gas constant (8.314 J mol^{-1} K^{-1}), and T is the absolute temperature of the reaction (K). Considering that constant heating rates were set, the relationship between time (t), temperature (T), and heating rate (β) can be described as

$$\beta = \frac{dT}{dt}. \tag{4}$$

By combing Eqs. (1), (3), and (4), the decomposition rate can be described as:

$$\frac{d\alpha}{dT} = \frac{A}{\beta}e^{-\frac{E_a}{RT}}f(\alpha). \tag{5}$$

In this study, isoconversional methods were chosen to describe the kinetics of pyrolysis and calculate the apparent activation energy without any assumptions in the kinetic model. The most common isoconversional integral methods are the Flynn–Wall–Ozawa (FWO), Kissinger–Akahira–Sunose (KAS), and Starink methods. These methods can be expressed as follows [34–36]:

$$\text{FWO: } \lg\beta = lg\left(\frac{AE_a}{g(\alpha)R}\right) - 2.315 - 0.4567\frac{E_a}{RT}, \tag{6}$$

$$\text{KAS: } \ln\left(\frac{\beta}{T^2}\right) = ln\left(\frac{AR}{g(\alpha)E_a}\right) - \frac{E_a}{RT}, \tag{7}$$

$$\text{Starink: } \ln\left(\frac{\beta}{T^{1.92}}\right) = C_s - 1.008\frac{E_a}{RT}. \tag{8}$$

Based on the above equations, it can be observed that there is a linear relationship between $1/T$ and $\lg\beta$ (FWO method), $\ln[\beta/T^2]$ (KAS method), and $\ln[\beta/T^{1.92}]$ (Starink method), and the activation energy can be determined from the slope. In this study, the conversion rate α was selected in the range of $0.05 \le \alpha \le 0.95$ with intervals of 0.01.

The reaction model was determined using the Criado master plot, which can be obtained by multiplying the differential and integral of the reaction model. The equation for Criado master plot can be expressed as follows [37]:

$$\frac{z(\alpha)}{z(0.5)} = \left(\frac{T_\alpha}{T_{0.5}}\right)^2 \times \frac{\left(\frac{d\alpha}{dt}\right)_\alpha}{\left(\frac{d\alpha}{dt}\right)_{0.5}} = \frac{f(\alpha)g(\alpha)}{f(0.5)g(0.5)}. \tag{9}$$

The kinetic reaction models used in this study are summarized in Table S1. After determining the reaction model, the pre-exponential factor can be determined using the compensation effect [38]:

$$\ln A_j = aE_j + b, \tag{10}$$

where, a and b are the parameters of the compensation effect, which are evaluated using several pairs of A_j and E_j. By combing Eqs. (1) and (3), the A_j and E_j can be calculated by:

$$\ln\left(\frac{d\alpha}{dt}\right) = \ln\left[A_j f(\alpha)\right] - \frac{E_j}{RT}. \tag{11}$$

The values of $\ln\left[A_j f(\alpha)\right]_\alpha$ can be calculated from the intercept, and E_j can be calculated from the slope of the plot between $1/T$ and $\ln\left(\frac{d\alpha}{dt}\right)$. The correct pre-exponential factor A_0 can be determined using Eq. (10) by substituting the activation energy values obtained from the isoconversional methods.

Py–GC/MS measurements

Slow and fast pyrolysis tests were conducted using a multi-shot pyrolyzer (EGA/Py-3030D, Frontier Laboratories Ltd., Japan) combined with gas chromatography/mass spectrometry (GC/MS) (GC:7890, MS:5975, Agilent, USA) (Py–GC/MS) to analyze pyrolyzates. An Ultra ALLOY® Capillary Column+—5 (30 m length, 0.25 mm i.d., 0.25 μm film thickness of 95% polydimethylsiloxane and 5% poly-diphenyl dimethylsiloxane stationary phase, Frontier Laboratories Ltd., Japan) was employed, and helium was used as the carrier gas with a flow rate of 1 mL min^{-1}. In fast pyrolysis, the pyrolyzer was set to 300, 400, 500, 600, and 700 °C for 10 min. In slow pyrolysis, the pyrolyzer was heated from 50 to 700 °C at 5, 10, 20, 30, and 40 °C min^{-1}. Approximately 0.5 mg of sample was loaded and the pyrolysis products were trapped by a cryotrap until the reaction was completed. Thereafter, the cryotrap was removed and the products were transferred to the MS via the separation column. The inlet mode was chosen as split mode with a split ratio of 100:1 and an inlet temperature of 300 °C. The GC oven program was set: 40 °C (5 min) → 20 °C min^{-1} → 300 °C (10 min) → 10 °C min^{-1} → 310 °C (5 min). The mass spectrometer was set to scan mode, and the scanning range was set to m/z 10–600 at 70 eV. The MS transfer line temperature, MSD source temperature, and MS quadrupole temperature were 280, 230, and 150 °C, respectively. As it is not possible to collect the pyrolysis products and determine the yield of oil or gas, the peak area percentage was calculated to obtain the changes in pyrolysis products and can be expressed by the following formula:

$$C_i = \frac{A_i}{\sum A_i} \times 100\%, \tag{12}$$

where, A_i is the peak area of the target compound, $\sum A_i$ is the total area of all the peaks in the chromatogram, and C_i (area %) is the peak area of the target compound as a percentage of the total peak area. MSD ChemStation (version F.01.03.2357, Agilent, USA) software with the NIST17 library was installed to calculate the peak area values. All experiments were repeated three times to reduce errors.

Results and discussion

TGA and kinetic analysis

The TG and derivative thermogravimetry (DTG) curves of PLA and PHBH at different heating rates are shown in Fig. 1. The weight loss characteristics are presented in Table S2. It can be observed that the TG and DTG curves of PLA and PHBH showed similar trends for all heating

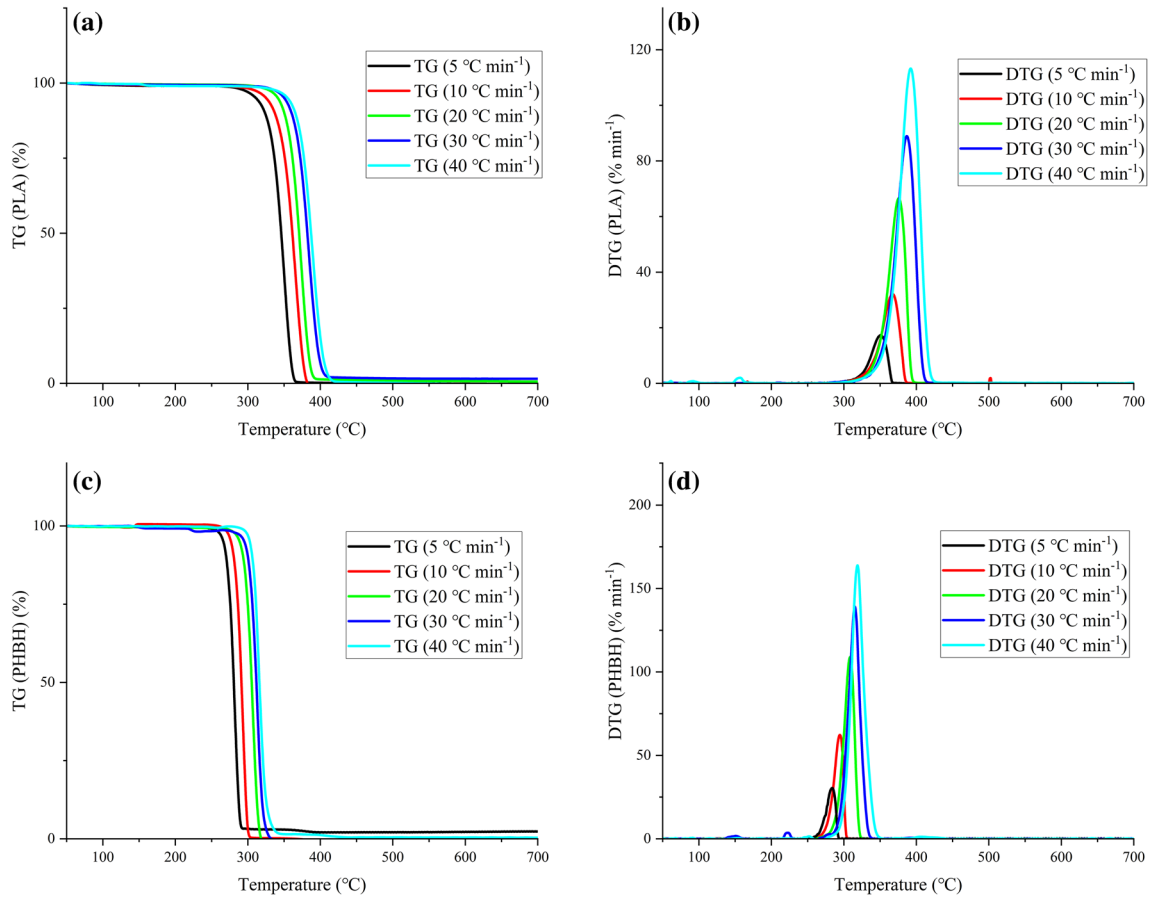

Fig. 1 **a** TG curves of PLA, **b** DTG curves of PLA, **c** TG curves of PHBH, **d** DTG curves of PHBH

rates, which indicated one-step weight loss. The thermal degradation of PLA started at 311–355 °C (5% mass fraction loss, $T_{5\%}$) and ended at 361–407 °C (95% mass fraction loss, $T_{95\%}$). The maximum mass loss of PLA occurred in the temperature range of 351–392 °C (T_{max}), with a decomposition rate range of 17.3–113.2 wt% min^{-1} (DTG_{max}). In the case of PHBH, the degradation was observed in the lower temperature range, which started at 266–303 °C and ended at 290–332 °C, and indicated that PLA was more stable than PHBH. These TG data are within the range reported in earlier studies. Gharsallah et al. [39] reported that the thermal degradation of PLA started at 300–342 °C and ended at 395–449 °C, and the maximum mass loss of PLA occurred in the temperature range of 345–394 °C when the heating rates were set to 5, 10, 20, and 40 °C min^{-1}. Li et al. [40] set the heating rates of PLA thermal degradation to 10, 15, 20, and 25 °C min^{-1} and observed that the start and end of temperature range were 334–356 °C and 368–386 °C, respectively. As for PHBH, Li et al. [41] reported that the thermal decomposition of PHBH started at 273 °C and ended at 304 °C, and the maximum mass loss occurred at 295 °C at a heating rate of 10 °C min^{-1}. At the end of thermal degradation, both PLA and PHBH lost nearly all the weight, and no residue was observed in the pan, which indicated that the thermal degradation of PLA and PHBH under nitrogen could be regarded as complete degradation. As the heating rate increased, the TG and DTG curves of PLA and PHBH shifted to higher temperatures, which can be explained by the thermal hysteresis effect and heat transfer limitations.

The apparent activation energies (E_a) of PLA and PHBH are shown in Fig. S1, and the linear correlation coefficient values are shown in Fig. S2. It can be observed that the E_a calculated by integral methods were similar, and showed similar tendency to the conversion values. The E_a of PLA were 161.1 ± 5.8 (FWO), 159.2 ± 6.0 (KAS), and 158.3 ± 5.9 (Starink). The three methods showed similar linear regressions, and the average correlation coefficients (R^2) of each method were 0.9902 ± 0.0053 (FWO), 0.9888 ± 0.0060 (KAS), and 0.9889 ± 0.0060 (Starink). In PHBH, the E_a were 146.0 ± 2.9 (FWO), 144.0 ± 3.1 (KAS), and 143.3 ± 3.0 (Starink). The average R^2 values of each method were 0.9980 ± 0.0008 (FWO), 0.9977 ± 0.0009 (KAS), and 0.9978 ± 0.0009 (Starink).

Due to the difference in samples, experimental conditions, and methodologies of kinetic analysis, the activation energy was reported in a wide range of studies. As shown in Table S3, the E_a value of commercial PLA was in the range of 140–180 kJ mol^{-1}. The synthesized PLA was reported in a wider range of 65–180 kJ mol^{-1} due to the difference in the manufacturing process and molecular weight. Few studies were conducted on the activation energy of PHBH pyrolysis and reported that the E_a value of commercial PHBH is 103–138 kJ mol^{-1}. The energy of the synthesized PHBH was reported to be in the range of 100–120 kJ mol^{-1}. Since PHBH is a copolymer, the activation energy was found to increase with increasing content of 3-hydroxyhexanoate [42]. Compared with the earlier data, the E_a values acquired in this study were at an intermediate level and very close to those reported using similar materials and methods. Comparing the integral methods, there was no significant difference between the E_a values calculated using the FWO, KAS, and Starink methods. Therefore, these three integral isoconversional methods are suitable for the kinetic calculations of PLA and PHBH.

In the Criado master plot method, the curve is considered unaffected by heating rates. Therefore, a heating rate of 20 °C min^{-1} was chosen as the representative to calculate the experimental plot. Figure 2 shows the Criado master plot of PLA and PHBH pyrolysis in the conversion range of 0.05–0.95 using experimental and theoretical data. The experimental plots of PLA and PHBH were well fitted with the R3 model. This indicated that nucleation occurs rapidly on the surface of the samples. The rate of degradation is controlled by the resulting reaction interface progress toward the center of the crystal. The mathematical model is different depending on the crystal shape, and R3 model represents the contracting sphere/cube (contracting volume) model, the sample particles have a spherical or cubical shape [43]. Experimental master plots of other heating rates could be found in Fig. S3 in the supplementary material, which were also well fitted with the R3 model. Similarly, kinetic models of many petroleum-based plastics were reported as geometrical contraction models, although they have simpler and oxygen-free structures [44]. The pre-exponential factors were calculated based on the kinetic method and are summarized in Table S4. The determined ln A_0 of PLA was 31.41 (FWO), 30.96 (KAS) and 30.13 (Starink). The PHBH values were 31.61 (FWO), 31.18 (KAS) and 31.01 (Starink). Similar to the activation energy results, the values of the pre-exponential factors did not show significant differences. Therefore, the activation energy and pre-exponential factor can be accurately determined using any of these three methods.

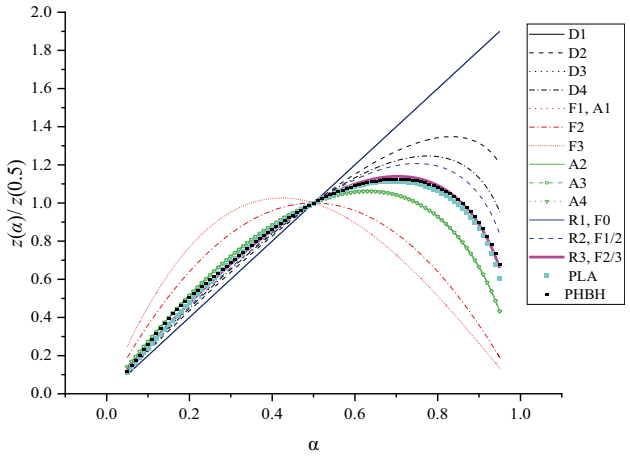

Fig. 2 Theoretical and experimental Criado master plots. Note: D1—diffusion model (one-dimensional diffusion); D2—diffusion model (two-dimensional diffusion); D3—diffusion model (three-dimensional diffusion (Jander)); D4—diffusion model (three-dimensional diffusion (Ginstling–Brounshtein)); F1—order-based model (first order); F2—order-based model (second order); F3—order-based model (third order); A2—Avrami–Erofeev model (random nucleation and nuclei growth: $n=1/2$, $m=2$); A3—Avrami–Erofeev model (random nucleation and nuclei growth: $n=1/3$, $m=3$); A4—Avrami–Erofeev model (random nucleation and nuclei growth: $n=1/4$, $m=4$); R1—geometrica contraction model (contracting disk); R2—geometrica contraction model (contracting cylinder); R3—geometrica contraction model (contracting sphere); PLA—experimental plot of PLA pyrolysis at 20 °C min^{-1}; PHBH—experimental plot of PHBH pyrolysis at 20 °C min^{-1}. Expressions for each reaction model are summarized in Table S1

Py–GC/MS analysis

Identification of pyrolysis products

Pyrolysis of PLA and PHBH was carried out using Py–GC/MS by fast and slow pyrolysis to study the types of products during the pyrolysis process. Due to the slow decomposition of PLA at 300 °C, the initial temperature of fast pyrolysis was increased to 350 °C. Although the pyrolysis temperature and heating rates were different, the number of main chromatographic peaks was the same. This indicates that the types of pyrolyzates obtained using the different heating methods were similar. Figure 3 shows the total ion chromatograms of PLA and PHBH from slow pyrolysis at a heating rate of 20 °C min^{-1} as a representative, and the peaks are numbered and listed. Major 9 peaks were observed during PLA pyrolysis. Peaks 1–4 were identified as acetaldehyde, lactic acid, meso-lactide, and D-, L-lactide, respectively, using the NIST17 library. Peaks 5–9 were considered cyclic lactide oligomers based on the research of Arrieta et al. [45]. In the total ion chromatograms of PHBH, 13 major peaks were observed, and peaks 1–5 were identified as propene, isocrotonic acid, crotonic acid, 2-hexenoic acid, and crotonic anhydride,

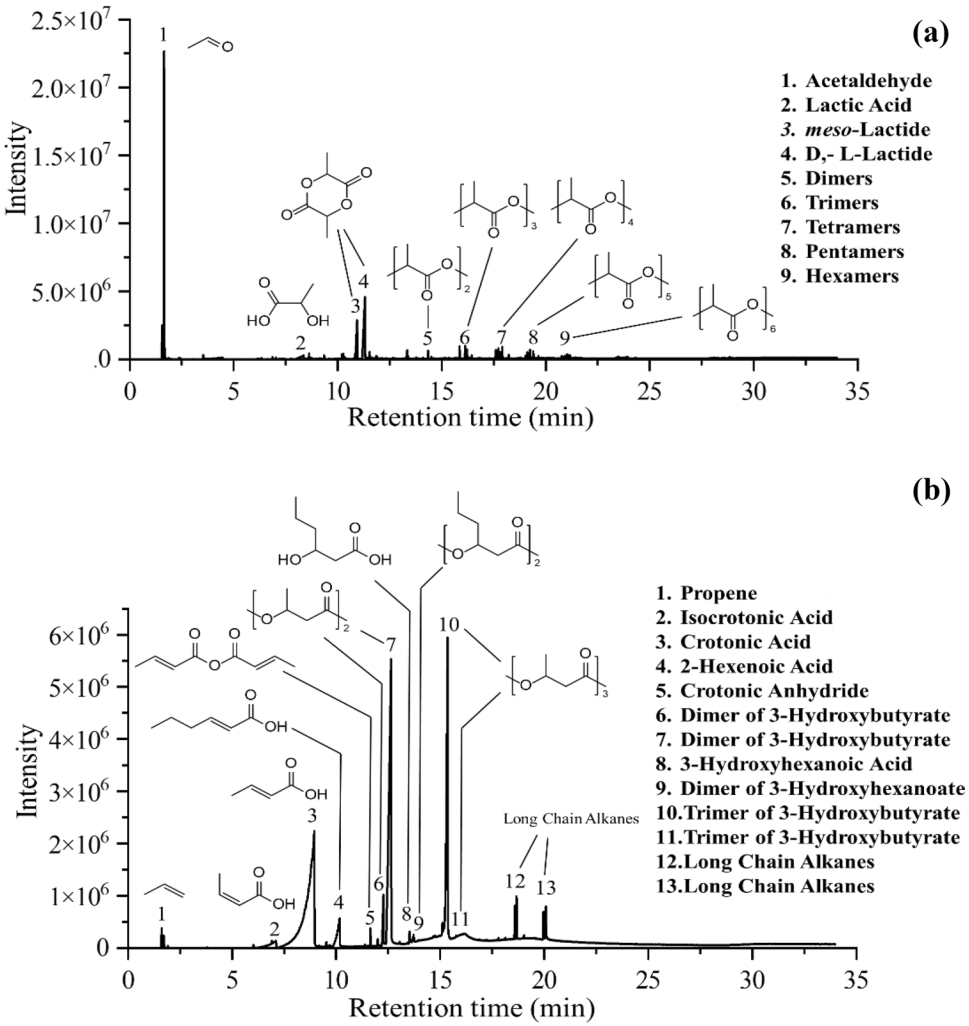

Fig. 3 The total ion chromatogram of **a** PLA, **b** PHBH at a heating rate of 20 °C min^{-1}

respectively, using the NIST17 library. According to earlier studies, peaks 6 and 7 were identified as dimers of 3-hydroxybutyrate; peaks 10 and 11 were identified as trimers of 3-hydroxybutyrate [21, 46]. Peaks 8 and 9 were identified as 3-hydroxyhexanoic acid and dimers of 3-hydroxyhexanoate, respectively, and their mass spectra are shown in Fig. S4. Although the data of their mass spectra were not found in the NIST library and literature, it can be observed that the mass spectrum of peak 8 showed a molecular ion at m/z 131 and fragment ions at $m/z = 69$, 87, and 114 from the fracture of the C–C and C–O links. A similar compound was observed by detecting methyl 3-methoxyhexanoate, the methyl derivative of 3-hydroxyhexanoic acid, using thermally assisted hydrolysis and methylation-gas chromatography [47]. The molecular ion was not identified in the mass spectrum of peak 9. However, fragment ions resulting from the McLafferty rearrangement of carboxyl and cleavage of C–C and C–O links were observed at $m/z = 55$, 69, 97, 114, and 182 [48, 49].

Among the products of PLA pyrolysis, lactide is remarkable as it is a raw material for the synthesis of PLA. The direct recovery of lactide is an advantage of PLA pyrolysis. Due to its poor compatibility with other pyrolysis oils and high melting point, lactide and crotonic acid existed in a solid state in the pyrolysis oil. Therefore, only a simple physical separation method is needed to separate the lactide or crotonic acid from the pyrolysis oil [50].

Effects of heating rates on the product distribution

The results of PLA slow pyrolysis were summarized in Fig. 4a. It can be observed that acetaldehyde, lactides, and oligomers were the main compounds at all heating rates, and a similar composition of PLA pyrolysis products is also reported [19, 50]. Approximately 14.5–29.6 area % of acetaldehyde was produced at different heating rates. As the most valuable chemical among the pyrolysis products, about 28.6–33.0 area % of lactides were generated, which includes meso-lactide (9.8–11.4 area %) and D-, L-lactide (18.8–21.8

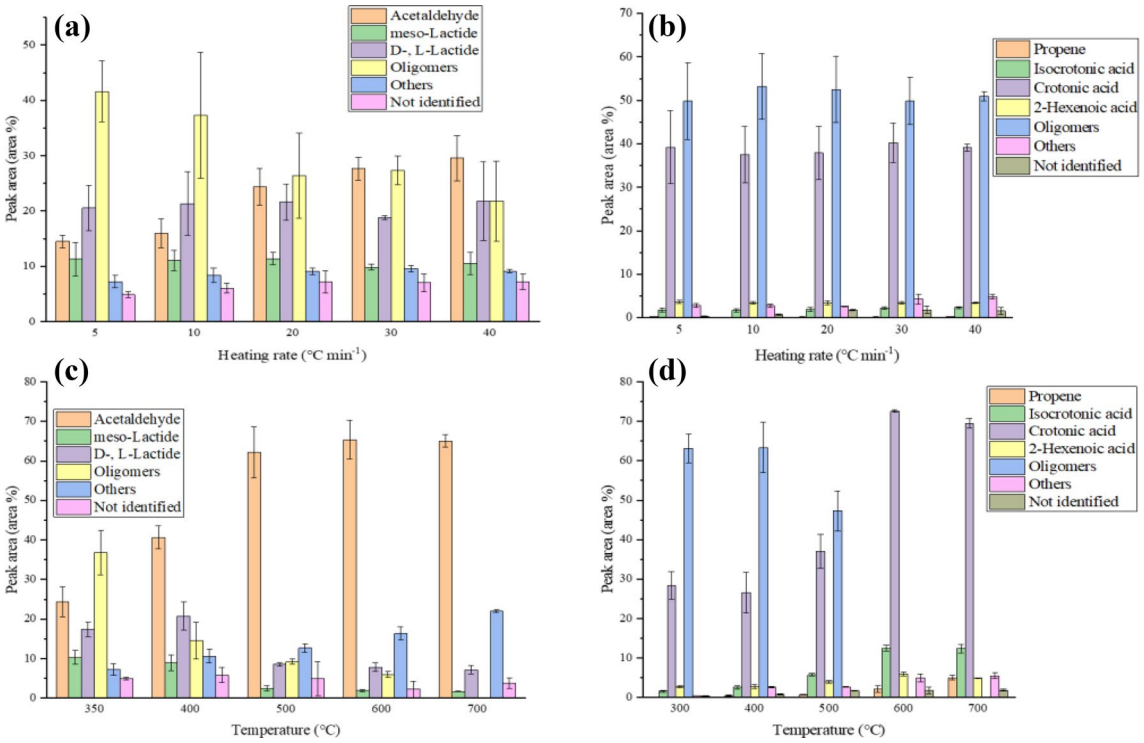

Fig. 4 Product distribution of **a** PLA slow pyrolysis, **b** PHBH slow pyrolysis, **c** PLA fast pyrolysis, **d** PHBH fast pyrolysis

area %), and D-, L-lactide was about twice that of meso-lactide. As previously mentioned, trans-esterification and free-radical are the main reactions in PLA pyrolysis, and acetaldehyde and CO are specific products of trans-esterification, whereas meso-lactide is a specific product of a radical reaction [19]. However, the current GC/MS configuration does not allow the isolation of CO, and it was not considered in this study. As the main products of PLA pyrolysis, the content of oligomers was 21.8–41.6 area %. Among the oligomers, tetramers were the highest, and approximately 6.2–10.3 area % of tetramers were produced. Additionally, CO_2, 2-propenoic acid, and lactic acid were detected at all the heating rates. Considering the low level, these compounds were summarized as "Others", which accounted for 7.2–9.5 area %. Although currently there are not many reports on the slow pyrolysis of PLA at different heating rates, the results obtained in this research are comparable with those of some studies that used a single heating rate. Nishida et al. [51] pyrolyzed PLA at a heating rate of 9 °C min^{-1} in the temperature range of 40–400 °C and reported that the intensity ratio of meso-form to total lactide was 36.8%. Mori et al. [52] heated PLA from 60 to 400 °C at a heating rate of 10 °C min^{-1} and observed that the peak areas of meso-lactide and D-, L-lactide were approximately 15 and 27%, respectively, of the total intensity. In this study, the intensity ratio of meso-form to total lactides was 34.1% and the peak area percentages of meso-lactide and D-, L-lactide were 11.0 and 21.3%, respectively, at a heating rate of 10 °C min^{-1}, which were quite similar to those in the earlier studies.

As the heating rate increased, the relative acetaldehyde content increased, and the number of oligomers decreased. However, there were no obvious regular lactide patterns. Acetaldehyde increased from 14.5 area % at 5 °C min^{-1} to 29.6 area % at 20 °C min^{-1}. While the oligomers decreased from 41.6 area % at 5 °C min^{-1} to 21.8 area % at 40 °C min^{-1}. Five types of oligomers (dimers, trimers, tetramers, pentamers, and hexamers) were identified at the heating rates of 20, 30, and 40 °C min^{-1}, but six types of oligomers, including octamers, were observed at 5 and 10 °C min^{-1}. Generally, in the slow pyrolysis of regular plastics, long-chain compounds can be obtained at high heating rates due to the short heating period. However, our results showed that temperature seems to have a greater effect than heating period on the slow pyrolysis of PLA. The heating period at a low heating rate was longer, and the decomposition was observed at lower temperatures. The temperature difference may be insignificant during the thermal degradation of regular plastic; however, it is considered in the process of PLA pyrolysis, which occurs in a small temperature window. With increasing temperature, radical reactions are enhanced, which promotes the conversion of oligomers into acetaldehyde [19].

The main products generated from PHBH during slow pyrolysis are shown in Fig. 4b. The "Others" groups included CO_2, H_2O, acetaldehyde, 1-pentene, crotonic

anhydride, and some long-chain alkanes which may be derived from additives. The pyrolysis products obtained at the different heating rates were the same. Due to the low content of poly-3-hydroxyhexanoic in PHBH, only 3.4–3.6 area % of 2-hexenoic acid, 0.1–0.4 area % of 3-hydroxyhexanoic acid, and 0.1–0.6 area % of dimers from 3-hydroxyhexanoic acid were detected. Oligomers higher than trimers were not detected probably because secondary reactions occurred [53]. Most of the compounds were obtained from 3-hydroxybutyrate, such as crotonic acid (37.9–40.2 area %), dimers of 3-hydroxybutyrate (28.5–32.0 area %) and trimers of 3-hydroxybutyrate (17.6–23.6 area %). Although there are very few studies on the thermal decomposition of PHBH at different heating rates, some research on PHB pyrolysis was conducted. Ariffin et al. [54] heated PHB film samples from 40 to 270 °C at a heating rate of 9 °C min^{-1} and found that the peak area ratio of crotonic acid to oligomers was 41:59, which was quite similar to that of this study (42:58 at 10 °C min^{-1}). As the heating rate increased, no obvious change was observed in any of the PHBH pyrolysis products. This shows that heating rates may affect the resistance to mass or heat transfer between the PHBH particles, but there was no significant effect on the product distribution.

Effects of temperature on products distribution during fast pyrolysis

In fast pyrolysis at different temperatures, the types of pyrolysis products were similar to those obtained from slow pyrolysis. As Fig. 4c shows, with the temperature of PLA pyrolysis increasing from 350 to 600 °C, acetaldehyde increased from 24.4 to 65.4 area %. However, it slightly declined to 65.0 area % when the pyrolysis temperature was set to 700 °C. This could be attributed to the cracking of acetaldehyde at high temperatures. Lactide was observed to change in the reverse direction to acetaldehyde and it first increased from 27.8 area % at 350 °C to 29.7 area % at 400 °C, and then decreased to 8.9 area % with the increase in pyrolysis temperature from 400 to 700 °C. Additionally, meso-lactide decreased from 10.3 area % at 350 °C to 1.7 area % at 700 °C. Simultaneously, D-, L-lactide increased from 17.5 area % at 350 °C to 20.8 area % at 400 °C, and decreased to 7.2 area % when the pyrolysis temperature was 700 °C. The type and quantity of oligomers decreased significantly when the pyrolysis temperature was increased. It decreased from 36.8 area % at 350 °C to 6.0 area % at 600 °C, and disappeared completely when the pyrolysis temperature was set to 700 °C. Six types of oligomers were detected at 350 °C, whereas only four types of oligomers were detected at 600 °C. These results indicate that high temperatures greatly promote the decomposition of oligomers and lactides to acetaldehyde, which is in agreement with the results of earlier studies. Saeaung et al. [55] analyzed the liquid products obtained from PLA pyrolysis by GC/MS and found that the relative area of lactide decreased dramatically from 58 to 8% when the pyrolysis temperature increased from 400 to 600 °C. Furthermore, a series of studies showed that meso-lactide decreased from 10.1 to 6.8 area %, and D-, L-lactide decreased from 29.6 to 15.6 area % when pyrolysis temperature increased from 300 to 600 °C [50, 56, 57]. Although there are differences in the specific values due to the different pyrolysis and analysis conditions, the trends are consistent, which indicates that temperature is an important factor that affects the products of PLA pyrolysis.

A similar phenomenon was observed during the pyrolysis of PHBH. Figure 4d shows the main product distribution generated from PHBH fast pyrolysis. The pyrolysis products were similar to those obtained from the slow pyrolysis. Crotonic acid increased from 28.4 area % at 300 °C and reached the maximum of 72.6 area % at 600 °C. When the temperature rose to 700 °C, it decreased to 69.6 area %. It is proved that crotonic acid will decompose to propene at a high temperature [53, 58]. In this study, propene had a big increase when the temperature reached 700 °C, which showed that the decrease in crotonic acid was caused by its cracking. Similarly, isocrotonic acid and 2-hexenoic acid increased as the temperature rose to 600 °C and decreased at 700 °C, which may be due to the same reason. Although few studies compared the yield of PHBH pyrolysis products, some studies reported that approximately 28.2% of crotonic acid and 52.1% of oligomers could be retrieved at a single temperature of 450 °C [59], which was in the range of our results. Oligomers decreased when the temperature increased from 300 to 500 °C and was decomposed completely when the temperature was above 600 °C. A similar phenomenon was observed by Gonzalez et al. [53] in the pyrolysis of PHB.

Suggested pyrolysis pathways of PLA and PHBH under different heating conditions

The pyrolysis mechanism of PLA is studied extensively [19, 20, 23], which consists of non-radical (include transesterification and cis-elimination) and radical reaction, and the pyrolysis pathways of the reactions are summarized in Scheme 1a, b. Based on the peak area percentages of the pyrolysis products, shown in Fig. S5, it is clear that the pyrolysis pathways of PLA were affected by the heating conditions. As shown in the schemes, CO and acetaldehyde are specific products of non-radical reactions. Among the pyrolysis products of PLA, the amount of acetaldehyde was remarkable, indicating that reaction (1) was the main reaction in both fast and slow pyrolysis. As the pyrolysis temperature and heating rate increased, this reaction strengthened significantly due to the increasing peak area percentage of acetaldehyde. Hence, the peak area percentage of the oligomers decreased simultaneously. However, as shown in

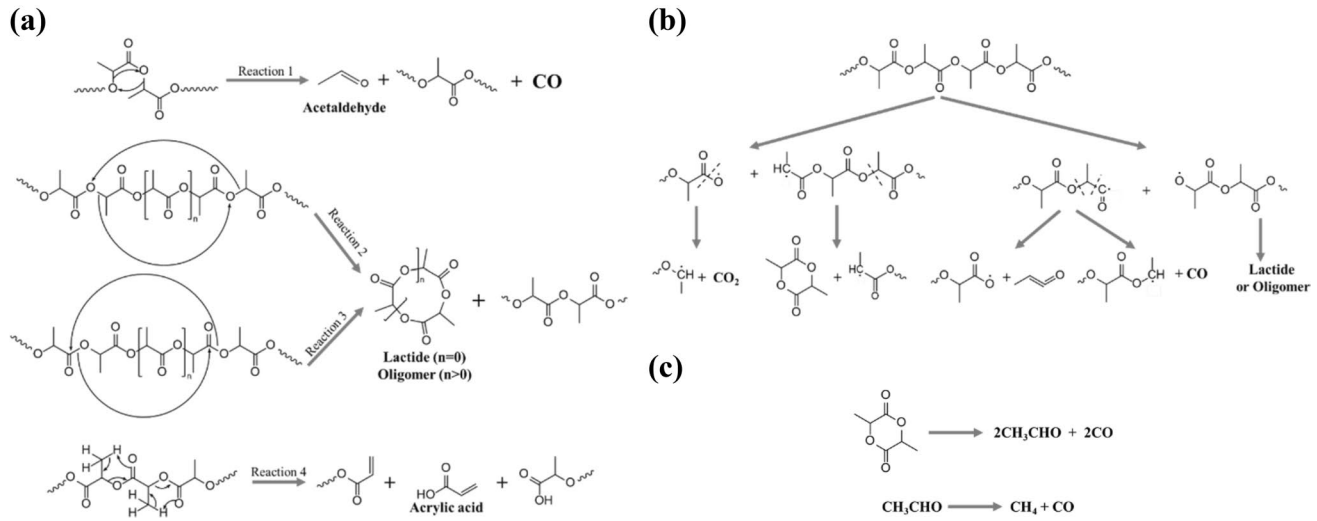

Scheme 1 The pyrolysis mechanism of PLA **a** non-radical reactions, **b** radical reactions, and **c** secondary reactions

Fig. 4 and Fig. S5, the amount of meso-lactide, D-, L-lactide, and CO_2 barely changed during the PLA slow pyrolysis process, which indicates that the limited temperature difference caused by the heating rate has little effect on reactions (2) and (3) in the non-radical and radical reactions. In the process of PLA fast pyrolysis, the peak area percentage of acetaldehyde and CO_2 increased significantly with an increase in temperature, indicating that both non-radical and radical reactions were enhanced. However, secondary reactions also contribute greatly, especially at temperatures above 500 °C. Scheme 1c summarizes the possible secondary reactions of the PLA pyrolysis products. As explained in the precious sections, lactide increased when the pyrolysis temperature increased from 350 to 400 °C, and rapidly decreased when the pyrolysis temperature was 500 °C. This suggests that secondary reactions will be promoted more than non-radical and radical reactions when pyrolysis temperature is above 500 °C. In the temperature range of 350–400 °C, D-, L-lactide increased, but meso-lactide decreased. This may be caused by the stability of different lactides. Generally, meso-lactide will decompose more; therefore, the secondary reaction of the specific product generated from radical reaction is stronger at 400 °C. The secondary reaction of acetaldehyde was limited because of the small reduction in peak area percentage at 700 °C. Conclusively, temperature is an important factor promoting the decomposition of PLA, but secondary reactions prevent from obtaining more lactide by increasing the temperature.

It was determined that β-elimination is the basic pyrolysis mechanism of poly-3-hydroxybutyrate, and anhydride production was reported as an additional mechanism [60, 61]. Although there is little research on the pyrolysis pathway of PHBH, considering the types of pyrolysis products, poly-3-hydroxyhexanoate (3Hx) may have similar pathways to poly-3-hydroxybutyrate (3HB) for decomposition through pyrolysis. The expected pyrolysis pathways for PHBH are summarized in Scheme 2a. However, trimers were observed only in the 3HB units. In this study, 3-hydroxyhexanoic acid, which was reported as a hydrolysate of 3-hydroxyhexanoate, was detected as a pyrolysis product. Therefore, there were differences between the pyrolysis pathways of the 3HB and 3Hx units. This may be caused by the side chains which can impede the formation of ring ester intermediates [61, 62]. The possible reaction pathway is shown in Scheme 2b. The water needed in this reaction may originate from anhydride production or dehydration of hydroxyl groups. As shown in Fig. S6, in slow pyrolysis, the pyrolysis pathways of PHBH were barely affected by the heating rates, as the peak area percentage of the main slow pyrolysis products varied little. In fast pyrolysis, the depolymerization of PHBH was accelerated with increasing temperature. The peak area percentages of crotonic and hexenoic acids increased significantly. As the temperature increased from 300 to 600 °C, the oligomers were further converted to monomers and eventually disappeared. In the temperature range of 300–500 °C, the production of crotonic anhydride and hydroxyhexanoic acid barely changed. However, it was significantly inhibited when the temperature was above 600 °C. Simultaneously, as more energy is obtained at high temperatures, secondary reactions are observed more clearly revealing that croton acid can be broken down into propylene and CO_2, whereas 2-hexenoic acid can be decomposed into 1-pentene and CO_2 which were detected and classified into "Others" group in the precious sections. As shown in Fig. S6, these compounds increased significantly, indicating that the secondary reactions were enhanced by the temperature. While at 700 °C, the adverse effects of secondary reactions were more obvious, resulting in a decrease in crotonic and hexenoic acids. Generally, the

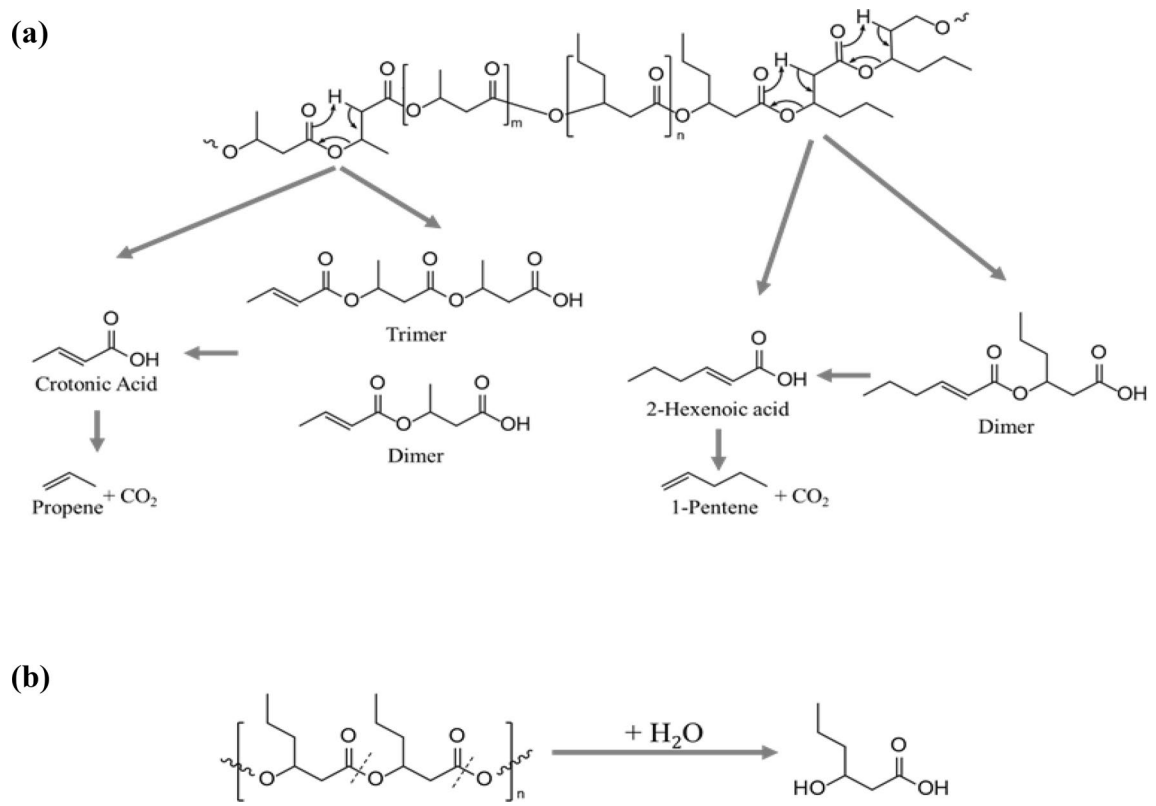

Scheme 2 Possible pathways of **a** PHBH pyrolysis, **b** formation of 3-hydroxyhexanoic acid

β-elimination reaction is dominant in the thermal decomposition of PHBH and can be enhanced by increasing temperature. The critical temperature is 600 °C because oligomers, anhydrides, and hydroxyhexanoic acids are not available. Simultaneously, the effects of the secondary reactions are also acceptable.

Conclusions

In this study, the effects of heating rate and temperature on the product distribution of slow (5, 10, 20, 30, and 40 °C min^{-1}) and fast pyrolysis (300, 400, 500, 600, and 700 °C) were investigated. The results show that temperature has a greater effect than heating rates on the pyrolysis product distribution of PLA and PHBH. As high-value chemicals, both high and low temperatures adversely affect the yield of lactide. In this study, fast pyrolysis at 400 °C is considered to be a suitable condition for lactides production, of which 29.7 area % of it was obtained. Unlike PLA, PHBH can be easily recovered by pyrolysis without catalysts, and fast pyrolysis at 600 °C is a suitable condition for obtaining crotonic acid with a maximum of 72.6 area %. Based on the characteristics of the PLA and PHBH pyrolysis, it is clear that the pyrolysis products are sensitive to temperature. Therefore, the pyrolysis temperature should be precisely controlled during the recovery of PLA and PHBH.

Supplementary Information The online version contains supplementary material available at https://doi.org/10.1007/s10163-022-01573-9.

Acknowledgements This research was supported by the Environment Research and Technology Development Fund [JPMEERF21511901] of the Environmental Restoration and Conservation Agency of Japan. We would also like to thank Kaneka Co. Ltd. for supplying the PHBH samples.

Data availability Data will be made available on request.

Declarations

Conflict of interest The authors declare that they have no known competing financial interests or personal relationships that could have appeared to influence the work reported in this paper.

References

1. Plastics Europe (2020) Plastics—the facts 2020. Plastics Europe. https://plasticseurope.org/knowledge-hub/plastics-the-facts-2020/. Accessed 6 Jan 2021
2. Plastics Europe (2009) The compelling facts about plastics 2009—an analysis of European plastics production, demand and recovery for 2008. Plastics Europe. https://plasticseurope.org/wp-content/uploads/2021/10/2009-Compelling-facts.pdf. Accessed 6 Jan 2021
3. Clark JH (2017) From waste to wealth using green chemistry: the way to long term stability. Curr Opin Green Sustain Chem 8:10. https://doi.org/10.1016/j.cogsc.2017.07.008
4. Law KL, Starr N, Siegler TR, Jambeck JR, Mallos NJ, Leonard GH (2020) The United States' contribution of plastic waste to land and ocean. Sci Adv 6:eabd0288. https://doi.org/10.1126/sciadv.abd0288
5. The People's Government of Beijing Municipal (2020) Beijing action plan for plastic pollution control (2020–2025). The People's Government of Beijing Municipal. http://www.beijing.gov.cn/zhengce/zhengcefagui/202012/t20201225_2185594.html. Accessed 6 Jan 2022
6. Ministry of the Environment (Japan) (2021) Roadmap for bioplastics introduction. Ministry of the Environment (Japan). https://www.env.go.jp/recycle/roadmap_for_bioplastics_introduction.html. Accessed 6 Jan 2021
7. European Bioplastics (2020) Bioplastics Market Development update 2020. In: 15th European bioplastics conference
8. Flury M, Narayan R (2021) Biodegradable plastic as an integral part of the solution to plastic waste pollution of the environment. Curr Opin Green Sustain Chem. https://doi.org/10.1016/j.cogsc.2021.100490
9. Mahadi Z, Yahya EA, Amin L, Yaacob M, Sino H (2021) Investigating Malaysian stakeholders' perceptions of the government's aim to replace conventional plastic bags with biodegradable and compostable bioplastic bags. J Mater Cycles Waste Manag 23:2133. https://doi.org/10.1007/s10163-021-01278-5
10. Ohtaki A, Nakasaki K (2000) Comparison of the weight-loss degradability of various biodegradable plastics under laboratory composting conditions. J Mater Cycles Waste Manag 2:118. https://doi.org/10.1007/s10163-000-0026-7
11. Dilkes-Hoffman LS, Lant PA, Laycock B, Pratt S (2019) The rate of biodegradation of PHA bioplastics in the marine environment: a meta-study. Mar Pollut Bull 142:15. https://doi.org/10.1016/j.marpolbul.2019.03.020
12. Sintim HY, Bary AI, Hayes DG et al (2019) Release of micro- and nanoparticles from biodegradable plastic during in situ composting. Sci Total Environ 675:686. https://doi.org/10.1016/j.scitotenv.2019.04.179
13. Honus S, Kumagai S, Fedorko G, Molnar V, Yoshioka T (2018) Pyrolysis gases produced from individual and mixed PE, PP, PS, PVC, and PET-Part I: production and physical properties. Fuel 221:346. https://doi.org/10.1016/j.fuel.2018.02.074
14. Kumagai S, Yoshioka T (2016) Feedstock recycling via waste plastic pyrolysis. J Jpn Petrol Inst 59:243. https://doi.org/10.1627/jpi.59.243
15. Lopez G, Artetxe M, Amutio M, Bilbao J, Olazar M (2017) Thermochemical routes for the valorization of waste polyolefinic plastics to produce fuels and chemicals. A review. Renew Sustain Energy Rev 73:346. https://doi.org/10.1016/j.rser.2017.01.142
16. Lopez G, Artetxe M, Amutio M, Alvarez J, Bilbao J, Olazar M (2018) Recent advances in the gasification of waste plastics. A critical overview. Renew Sustain Energy Rev 82:576. https://doi.org/10.1016/j.rser.2017.09.032
17. Al-Salem SM, Antelava A, Constantinou A, Manos G, Dutta A (2017) A review on thermal and catalytic pyrolysis of plastic solid waste (PSW). J Environ Manag 197:177. https://doi.org/10.1016/j.jenvman.2017.03.084
18. Kumagai S, Nakatani J, Saito Y, Fukushima Y, Yoshioka T (2020) Latest trends and challenges in feedstock recycling of polyolefinic plastics. J Jpn Petrol Inst 63:345. https://doi.org/10.1627/jpi.63.345
19. Kopinke FD, Remmler M, Mackenzie K, Moder M, Wachsen O (1996) Thermal decomposition of biodegradable polyesters. 2. Poly(lactic acid). Polym Degrad Stab 53:329. https://doi.org/10.1016/0141-3910(96)00102-4
20. Kopinke FD, Mackenzie K (1997) Mechanistic aspects of the thermal degradation of poly(lactic acid) and poly(beta-hydroxybutyric acid). J Anal Appl Pyrolysis 40–1:43. https://doi.org/10.1016/s0165-2370(97)00022-3
21. Kopinke FD, Remmler M, Mackenzie K (1996) Thermal decomposition of biodegradable polyesters. 1. Poly(beta-hydroxybutyric acid). Polym Degrad Stab 52:25. https://doi.org/10.1016/0141-3910(95)00221-9
22. Wang XJ, Huang Z, Wei MY et al (2019) Catalytic effect of nanosized ZnO and TiO_2 on thermal degradation of poly(lactic acid) and isoconversional kinetic analysis. Thermochim Acta 672:14. https://doi.org/10.1016/j.tca.2018.12.008
23. Feng LD, Feng SY, Bian XC, Li G, Chen XS (2018) Pyrolysis mechanism of poly(lactic acid) for giving lactide under the catalysis of tin. Polym Degrad Stab 157:212. https://doi.org/10.1016/j.polymdegradstab.2018.10.008
24. Ariffin H, Nishida H, Hassan MA, Shirai Y (2010) Chemical recycling of polyhydroxyalkanoates as a method towards sustainable development. Biotechnol J 5:484. https://doi.org/10.1002/biot.200900293
25. Ariffin H, Nishida H, Shirai Y, Hassan MA (2010) Highly selective transformation of poly(R)-3-hydroxybutyric acid into trans-crotonic acid by catalytic thermal degradation. Polym Degrad Stab 95:1375. https://doi.org/10.1016/j.polymdegradstab.2010.01.018
26. Pan R, Martins MF, Debenest G (2022) Interactions of operating parameters on the production of waste polypropylene pyrolysis oil: neural fuzzy model and genetic algorithm optimization. J Mater Cycles Waste Manag. https://doi.org/10.1007/s10163-022-01521-7
27. Dutta N, Mondal P, Gupta A (2022) Optimization of process parameters using response surface methodology for maximum liquid yield during thermal pyrolysis of blend of virgin and waste high-density polyethylene. J Mater Cycles Waste Manag 24:1182. https://doi.org/10.1007/s10163-022-01392-y
28. López A, de Marco I, Caballero BM, Laresgoiti MF, Adrados A (2011) Influence of time and temperature on pyrolysis of plastic wastes in a semi-batch reactor. Chem Eng J 173:62. https://doi.org/10.1016/j.cej.2011.07.037
29. Singh RK, Ruj B, Sadhukhan AK, Gupta P (2019) Impact of fast and slow pyrolysis on the degradation of mixed plastic waste: product yield analysis and their characterization. J Energy Inst 92:1647. https://doi.org/10.1016/j.joei.2019.01.009
30. Kumagai S, Yoshioka T (2021) Chemical feedstock recovery from hard-to-recycle plastics through pyrolysis-based approaches and pyrolysis–gas chromatography. Bull Chem Soc Jpn 94:2370. https://doi.org/10.1246/bcsj.20210219

31. Kumagai S, Yoshioka T (2021) Latest trends in pyrolysis gas chromatography for analytical and applied pyrolysis of plastics. Anal Sci 37:145. https://doi.org/10.2116/analsci.20SAR04
32. Westphal C, Perrot C, Karlsson S (2001) Py–GC/MS as a means to predict degree of degradation by giving microstructural changes modelled on LDPE and PLA. Polym Degrad Stab 73:281. https://doi.org/10.1016/s0141-3910(01)00089-1
33. Li SD, He JD, Yu PH, Cheung MK (2003) Thermal degradation of poly(3-hydroxybutyrate) and poly(3-hydroxybutyrate-*co*-3-hydroxyvalerate) as studied by TG, TG-FTIR, and Py–GC/MS. J Appl Polym Sci 89:1530. https://doi.org/10.1002/app.12249
34. Ozawa T (1992) Estimation of activation-energy by isoconversion methods. Thermochim Acta 203:159. https://doi.org/10.1016/0040-6031(92)85192-x
35. Kissinger HE (1956) Temperature with heating rate in differential thermal analysis. J Res Natl Bur Stand 57:217. https://doi.org/10.6028/jres.057.026
36. Starink MJ (2003) The determination of activation energy from linear heating rate experiments: a comparison of the accuracy of isoconversion methods. Thermochim Acta 404:163. https://doi.org/10.1016/s0040-6031(03)00144-8
37. Criado JM, Malek J, Ortega A (1989) Applicability of the master plots in kinetic-analysis of non-isothermal data. Thermochim Acta 147:377. https://doi.org/10.1016/0040-6031(89)85192-5
38. Vyazovkin S (1996) A unified approach to kinetic processing of nonisothermal data. Int J Chem Kinet 28:95. https://doi.org/10.1002/(sici)1097-4601(1996)28:2%3c95::Aid-kin4%3e3.0.Co;2-g
39. Gharsallah A, Layachi A, Louaer A, Satha H (2021) Thermal degradation kinetics of Opuntia Ficus Indica flour and talc-filled poly(lactic acid) hybrid biocomposites by TGA analysis. J Compos Mater 55:3099. https://doi.org/10.1177/00219983211008202
40. Li J, Zheng W, Li L, Zheng Y, Lou X (2009) Thermal degradation kinetics of g-HA/PLA composite. Thermochim Acta 493:90. https://doi.org/10.1016/j.tca.2009.04.009
41. Li DN, Fu JR, Ma XJ (2020) Improvement in thermal, mechanical, and barrier properties of biocomposite of poly(3-hydroxybutyrate-*co*-3-hydroxyhexanoate)/modified nano-SiO_2. Polym Compos 41:381. https://doi.org/10.1002/pc.25377
42. Asrar J, Valentin HE, Berger PA, Tran M, Padgette SR, Garbow JR (2002) Biosynthesis and properties of poly(3-hydroxybutyrate-*co*-3-hydroxyhexanoate) polymers. Biomacromol 3:1006. https://doi.org/10.1021/bm025543a
43. Khawam A, Flanagan DR (2006) Solid-state kinetic models: basics and mathematical fundamentals. J Phys Chem B 110:17315. https://doi.org/10.1021/jp062746a
44. Aboulkas A, El Harfi K, El Bouadili A (2010) Thermal degradation behaviors of polyethylene and polypropylene. Part I: pyrolysis kinetics and mechanisms. Energy Convers Manag 51:1363. https://doi.org/10.1016/j.enconman.2009.12.017
45. Arrieta MP, Parres F, Lopez J, Jimenez A (2013) Development of a novel pyrolysis-gas chromatography/mass spectrometry method for the analysis of poly(lactic acid) thermal degradation products. J Anal Appl Pyrolysis 101:150. https://doi.org/10.1016/j.jaap.2013.01.017
46. Sato H, Hoshino M, Aoi H et al (2005) Compositional analysis of poly(3-hydroxybutyrate-*co*-3-hydroxyvalerate) by pyrolysis-gas chromatography in the presence of organic alkali. J Anal Appl Pyrolysis 74:193. https://doi.org/10.1016/j.jaap.2004.12.011
47. Baiduran S, Murugan P, Sen KY et al (2019) Evaluation of soil burial biodegradation behavior of poly(3-hydroxybutyrate-*co*-3-hydroxyhexanoate) on the basis of change in copolymer composition monitored by thermally assisted hydrolysis and methylation-gas chromatography. J Anal Appl Pyrolysis 137:146. https://doi.org/10.1016/j.jaap.2018.11.020
48. Gross JH (2017). In: Gross JH (ed) Mass spectrometry: a textbook. Springer International Publishing, Cham
49. Sparkman OD, Penton ZE, Kitson FG (2011). In: Sparkman OD, Penton ZE, Kitson FG (eds) Gas chromatography and mass spectrometry, 2nd edn. Academic Press, Amsterdam
50. Sun C, Chen XJ, Zheng DY et al (2021) Exploring the synergetic effects of the major components of biomass additives in the pyrolysis of polylactic acid. Green Chem 23:9014. https://doi.org/10.1039/d1gc03002g
51. Nishida H, Mori T, Hoshihara S, Fan YJ, Shirai Y, Endo T (2003) Effect of tin on poly(L-lactic acid) pyrolysis. Polym Degrad Stab 81:515. https://doi.org/10.1016/s0141-3910(03)00152-6
52. Mori T, Nishida H, Shirai Y, Endo T (2004) Effects of chain end structures on pyrolysis of poly(L-lactic acid) containing tin atoms. Polym Degrad Stab 84:243. https://doi.org/10.1016/j.polymdegradstab.2003.11.008
53. Gonzalez A, Irusta L, Fernandez-Berridi MJ, Iriarte M, Iruin JJ (2005) Application of pyrolysis/gas chromatography/Fourier transform infrared spectroscopy and TGA techniques in the study of thermal degradation of poly(3-hydroxybutyrate). Polym Degrad Stab 87:347. https://doi.org/10.1016/j.polymdegradstab.2004.09.005
54. Ariffin H, Nishida H, Shirai Y, Hassan MA (2009) Anhydride production as an additional mechanism of poly(3-hydroxybutyrate) pyrolysis. J Appl Polym Sci 111:323. https://doi.org/10.1002/app.29034
55. Saeaung K, Phusunti N, Phetwarotai W, Assabumrungrat S, Cheirsilp B (2021) Catalytic pyrolysis of petroleum-based and biodegradable plastic waste to obtain high-value chemicals. Waste Manag (Oxford) 127:101. https://doi.org/10.1016/j.wasman.2021.04.024
56. Sun C, Li CX, Tan HY, Zhang YH (2019) Synergistic effects of wood fiber and polylactic acid during co-pyrolysis using TG–FTIR–MS and Py–GC/MS. Energy Convers Manag 202:12. https://doi.org/10.1016/j.enconman.2019.112212
57. Sun C, Li W, Chen X, Li C, Tan H, Zhang Y (2021) Synergistic interactions for saving energy and promoting the co-pyrolysis of polylactic acid and wood flour. Renew Energy 171:254. https://doi.org/10.1016/j.renene.2021.02.099
58. Clark JM, Pilath HM, Mittal A, Michener WE, Robichaud DJ, Johnson DK (2016) Direct production of propene from the thermolysis of poly(beta-hydroxybutyrate) (PHB). An experimental and DFT investigation. J Phys Chem A 120:332. https://doi.org/10.1021/acs.jpca.5b09246
59. Cornelissen T, Molenberghs G, Jans M, Yperman J, Schreurs S, Carleer R (2012) A statistical data-processing methodology of Py–GC/MS data for the simulation of flash co-pyrolysis reactor experiments. Chemom Intell Lab Syst 110:123. https://doi.org/10.1016/j.chemolab.2011.10.011
60. Xiang HX, Wen XS, Miu XH, Li Y, Zhou Z, Zhu MF (2016) Thermal depolymerization mechanisms of poly(3-hydroxybutyrate-*co*-3-hydroxyvalerate). Prog Nat Sci Mater Int 26:58. https://doi.org/10.1016/j.pnsc.2016.01.007
61. Sin MC, Gan SN, Annuar MSM, Tan IKP (2010) Thermodegradation of medium-chain-length poly(3-hydroxyalkanoates) produced by *Pseudomonas putida* from oleic acid. Polym Degrad Stab 95:2334. https://doi.org/10.1016/j.polymdegradstab.2010.08.027
62. Rajaratanam DD, Ariffin H, Hassan MA, Kawasaki Y, Nishida H (2017) Effects of (R)-3-hydroxyhexanoate units on thermal hydrolysis of poly((R)-3-hydroxybutyrate-*co*-(R)-3-hydroxyhexanoate)s. Polym Degrad Stab 137:58. https://doi.org/10.1016/j.polymdegradstab.2017.01.007